



## Structural phase transitions in $\text{Zn}(\text{CN})_2$ under high pressures

H.K. Poswal<sup>a,\*</sup>, A.K. Tyagi<sup>b</sup>, Andrea Lausi<sup>c</sup>, S.K. Deb<sup>a</sup>, Surinder M. Sharma<sup>a</sup>

<sup>a</sup> High Pressure Physics Division, Bhabha Atomic Research Centre, Trombay, Mumbai 400085, India

<sup>b</sup> Chemistry Division, Bhabha Atomic Research Centre, Trombay, Mumbai 400085, India

<sup>c</sup> Synchrotron Trieste-Elettra, S. S. -14 Km 163, 5 in Area Science Park, 34012 Basovizza, Trieste, Italy

### ARTICLE INFO

#### Article history:

Received 13 June 2008

Received in revised form

25 September 2008

Accepted 29 September 2008

Available online 17 October 2008

#### Keywords:

High pressure

X-ray diffraction

Structural phase transition

Negative thermal expansion

### ABSTRACT

High pressure behavior of zinc cyanide ( $\text{Zn}(\text{CN})_2$ ) has been investigated with the help of synchrotron-based X-ray diffraction measurements. Our studies reveal that under pressure this compound undergoes phase transformations and the structures of the new phases depend on whether the pressure is hydrostatic or not. Under hydrostatic conditions,  $\text{Zn}(\text{CN})_2$  transforms from cubic to orthorhombic to cubic-II to amorphous phases. In contrast, the non-hydrostatic pressure conditions drive the ambient cubic phase to a partially disordered crystalline phase, which eventually evolves to a substantially disordered phase. The final disordered phase in the latter case is distinct from the amorphous phase observed under the hydrostatic pressures.

© 2008 Elsevier Inc. All rights reserved.

### 1. Introduction

Though the property of negative thermal expansion (NTE) is known for a long time, this topic got an impetus after the discovery of a large isotropic NTE in  $\text{Zr}(\text{WO}_4)_2$  over a wide range of temperature [1–5]. Aside from the interesting underlying physics, the research in this topic is also driven by the technological applications. For example some applications may require materials with pre-designed and small thermal expansion [6]. Generally such materials are engineered through an appropriate mixture of compounds having positive and NTE. In such a composite making process, grain interactions are subjected to local stresses. Thus it is desirable that the component compounds of the composite should not undergo any local stress-induced phase transformation which may substantially affect the thermal expansion behavior. In this context, the knowledge of the behavior of NTE compounds under pressure may be useful.

Many of the compounds displaying NTE are oxides having framework structures with a strong single-atom bridge, such as in  $A(\text{MO}_4)_2$ ,  $\text{AM}_2\text{O}_7$ ,  $\text{A}_2(\text{MO}_4)_3$  ( $A = \text{Zr, Hf, Sc, Lu, Al}$  etc.,  $M = \text{W, Mo, V}$ , etc.) and NASICON families of compounds [4,7,8]. High-pressure structural studies of these materials have shown that these undergo phase transitions to other crystalline phases at relatively low pressures, eventually becoming amorphous at higher pressures. For example, cubic  $\text{Zr}(\text{WO}_4)_2$ ,  $\text{Hf}(\text{WO}_4)_2$  and  $\gamma\text{-Zr}(\text{MoO}_4)_2$ , where the librational motion of both the constituent polyhedra

contribute to NTE [9], transform to other crystalline phases at 0.2, 0.6 GPa and over 0.7–2.5 GPa, respectively ([4] and reference therein). On the other hand, cubic  $\text{ZrV}_2\text{O}_7$ , wherein only the rotation of the  $\text{VO}_4$  contributes to NTE, transforms from cubic to an orthorhombic phase over  $\sim 1.4\text{--}1.7$  GPa [9]. A large number of anisotropic compounds ( $\text{Sc}_2(\text{WO}_4)_3$ ,  $\text{Lu}_2(\text{WO}_4)_3$ ,  $\text{Al}_2(\text{WO}_4)_3$ , and molybdates) [4,7,8] have also been studied under pressure with the help of X-ray diffraction as well as Raman and IR measurements and these too undergo transitions to crystalline phases before leading to pressure-induced amorphization (PIA) [10]. However, in spite of the fact that several compounds which show NTE at room pressure are known to become amorphous at high pressures, such a correlation may be coincidental. This is because the transformation to another crystalline phase may almost eliminate the NTE effect, as observed in  $\text{Zr}(\text{WO}_4)_2$  [11]. It is also interesting to note that molecular dynamics simulations have shown that model network systems have a tendency to become amorphous under compression [12].

Recently cyanide-based framework compounds have also been shown to have NTE [13–16]. Of these  $\text{Zn}(\text{CN})_2$  is the simplest coordination framework compound having a cubic crystal structure and an isotropic and large NTE coefficient ( $\approx$  twice that for  $\text{Zr}(\text{WO}_4)_2$ ) over a wide range of temperature. Structural analysis with the help of atomic pair distribution function implies that with the increase in the temperature, the transverse displacement of C–N bridge increases [17]. This compound is very flexible and soft as implied by the existence of low energy lattice vibrations [14,18–20].

The structure of  $\text{Zn}(\text{CN})_2$ , shown in Fig. 1, consists of two interpenetrating three dimensional tetrahedral framework made up of Zn–C–N–Zn chains. Zinc cyanide ( $\text{Zn}(\text{CN})_2$ ) may have either

\* Corresponding author. Fax: +91 222 550 5151.

E-mail addresses: [himanshu@barc.gov.in](mailto:himanshu@barc.gov.in), [poswalhimanshu@gmail.com](mailto:poswalhimanshu@gmail.com) (H.K. Poswal).

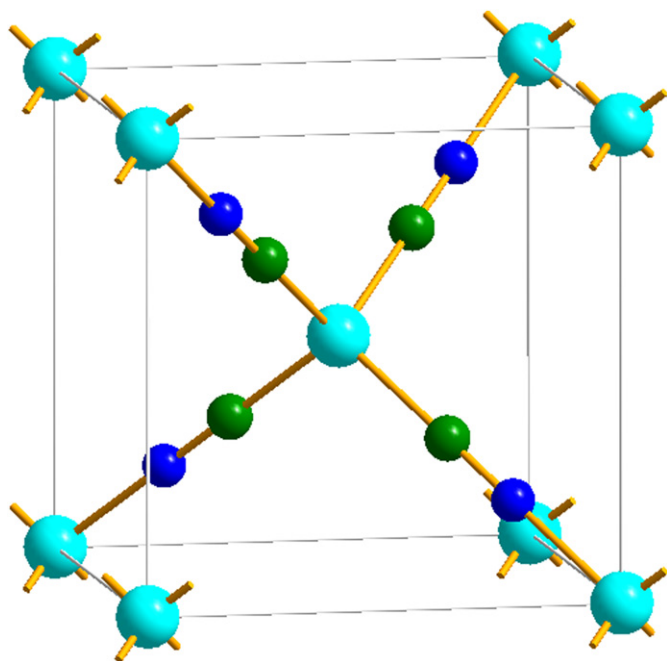


**Fig. 1.** Crystal structure of  $\text{Zn}(\text{CN})_2$  at ambient conditions (color online). Large (light blue) spheres at the vertices represent Zn. Other two smaller atoms (deep blue and green) are C and N. In the disordered structure the occupancy of each equivalent site by C and N is 1/2.

of the two probable cubic structures, the CN-ordered structure (space group  $P43m$ ) [15] and CN-disordered structure (space group  $Pn\bar{3}m$ ) [13]. In the ordered structure the C and N ions, lying along the body diagonal, are ordered such that they form alternate  $\text{ZnC}_4$  and  $\text{ZnN}_4$  tetrahedra. And in the disordered structure, statistically the site occupancy by C and N atoms is 0.5. Because of close values of X-ray atomic scattering factors, it is very difficult to differentiate between these two probable structures using X-ray diffraction technique. However, the thermal displacement analysis of neutron time-of-flight diffraction measurements favors the disordered structure [13]. Subsequent Raman and IR spectroscopic studies also support a disordered cubic structure for  $\text{Zn}(\text{CN})_2$  [21].

The present study aims to investigate the high pressure behavior of  $\text{Zn}(\text{CN})_2$ . Aside from the fact that pressure, and the consequent phase transitions, would affect the NTE behavior, it would also help identify the features common to other NTE compounds. Earlier high pressure studies ( $P \leq 2$  GPa) have provided some useful information. For example, Chapman and Chupas [22] have shown that (upto  $\sim 1$  GPa) pressure enhances NTE i.e.,  $\delta\alpha/\delta P \sim -5 \times 10^{-6} \text{K}^{-1}/\text{GPa}$ . Another investigation claims that this compound becomes almost amorphous at very low pressures,  $\sim 1.6$  GPa [23]. In this manuscript, we present the results of our high pressure angle dispersive X-ray diffraction measurements on  $\text{Zn}(\text{CN})_2$  employing synchrotron radiation.

## 2. Experimental details

$\text{Zn}(\text{CN})_2$  sample was synthesized employing precipitation technique using  $\text{ZnCl}_2$  and KCN solutions and the product was characterized to be  $\text{Zn}(\text{CN})_2$  with the help of X-ray diffraction measurements. For the high pressure experiments,  $\text{Zn}(\text{CN})_2$  was loaded in a tungsten gasket hole of  $\sim 120 \mu\text{m}$  diameter, drilled after pre-indenting it to a thickness of  $\sim 70 \mu\text{m}$  and mounted in a Mao-Bell kind of diamond-anvil cell (DAC). For pressure calibration a few particles of gold were also loaded in the gasket hole.

The experiments were performed in hydrostatic as well as non-hydrostatic pressure environments. For the studies under hydrostatic pressures, methanol: water mixture (16:3:1) was used as a pressure transmitting fluid which provides almost hydrostatic conditions up to  $\sim 15$  GPa [16]. For the experiments under non-hydrostatic conditions, no pressure transmitting fluid was used. The pressure was determined from the known equation of state of gold [24]. High-pressure angle dispersive X-ray diffraction experiments were carried out at the 5.2 R (XRD1) beamline of Elettra synchrotron source, with monochromatic X-rays of wavelength  $0.67019 \text{ \AA}$ . The diffraction patterns were recorded using MAR345 imaging plate detector kept at a distance of  $\sim 200$  mm from the sample. Two-dimensional imaging plate records were transformed to one dimensional diffraction profiles by the radial integration of diffraction rings using the FIT2D software [25].

## 3. Results and discussion

Fig. 2 shows one dimensional angle dispersive X-ray diffraction profiles of  $\text{Zn}(\text{CN})_2$  at a few representative pressures under hydrostatic conditions. Analysis of diffraction patterns indicates that  $\text{Zn}(\text{CN})_2$  remains in the cubic structure up to  $\sim 1$  GPa. The Rietveld refinement carried out on the diffraction pattern recorded at 0.4 GPa confirms the earlier difficulty in resolving CN-ordered form ( $P43m$ ) from the CN-disordered one ( $Pn\bar{3}m$ ) with

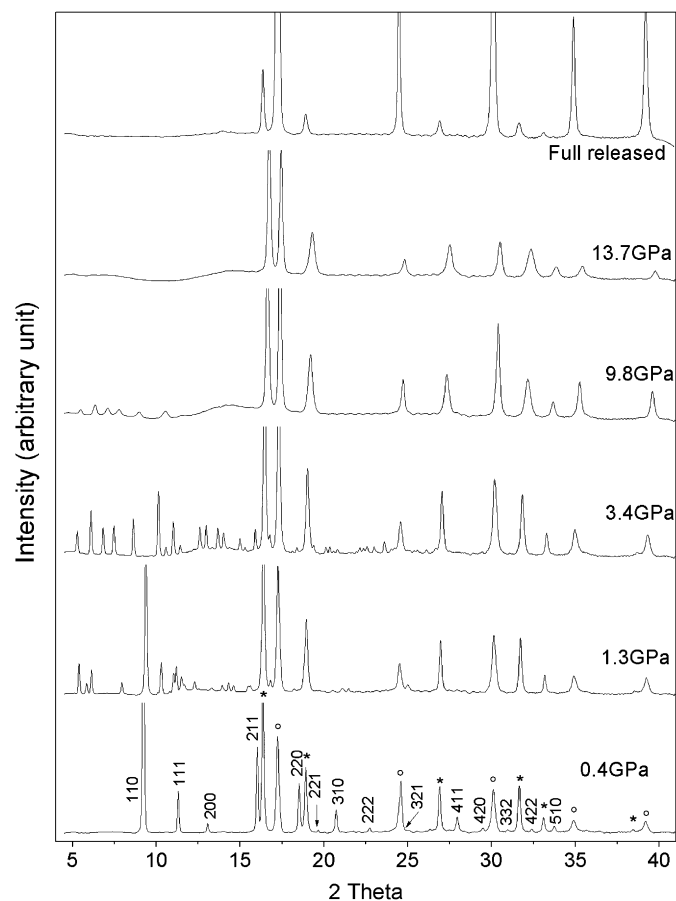


**Fig. 2.** X-ray diffraction patterns of  $\text{Zn}(\text{CN})_2$  at a few representative pressures under hydrostatic conditions. Open circles and asterisks represent the diffraction peaks from tungsten gasket and gold pressure marker, respectively.  $hkl$  indices are given only for the cubic  $\text{Zn}(\text{CN})_2$ .

the help of X-ray diffraction data. For the initial cubic phase, the variation of the lattice parameter was obtained by analyzing the diffraction patterns with the help of Le Bail profile fitting, as implemented in GSAS software [26]. From a very few  $P$ - $V$  data points obtained in the initial cubic phase, it is difficult to determine bulk modulus ( $B$ ) and its derivative ( $B'$ ). However, we find that our data are consistent with the results of Ref. [17] (i.e., with  $B = 34.19(21)$  GPa and  $B' = -6.0(7)$ ). On increase of pressure beyond 1 GPa many new diffraction peaks at higher  $d$ -values appeared. These observed changes indicate that the structure has transformed to a new high pressure phase, having larger lattice parameters. Coexistence of ambient phase with the high pressure phase implies the transformation to be of the first order. In order to index the high pressure phase, Crysfire software [27] was used which gave the new structure to be of orthorhombic symmetry and with lattice parameters,  $a = 4.109$ ,  $b = 7.113$  and  $c = 13.165$  Å at 1.3 GPa. Checkcell software [28] was used to obtain the best possible space group (consistent with extinction conditions) to be  $Pmc2_1$ . Fig. 3 shows that orthorhombic cell gives excellent Le Bail profile fitting of the experimental diffraction pattern. (The details of indexing with this orthorhombic cell are given as the supplementary information.) However, due to the observation of only a few diffraction peaks, the detailed structure of the new phase could not be determined. Density considerations suggest that each unit cell in the orthorhombic phase may have at least four formula units and this would imply  $\sim 5.9\%$  volume reduction per formula unit across the phase transition. This is consistent with the multiplicity of sites in  $Pmc2_1$  space group.

The diffractions patterns in Fig. 2 imply that the structure evolved to still another phase at  $\sim 2$  GPa. This could be indexed (using Crysfire software [27]) to be a cubic phase with a rather large lattice parameter, i.e.,  $a = 12.669$  Å at 2.5 GPa. As displayed in Fig. 4, three phase Le Bail profile refinement (i.e., with gold pressure marker, tungsten gasket and high pressure cubic phase) shows a very good fitting to the experimental data. (Details of this indexing too are submitted as supplementary information.) Here too, due to the limited number of observed diffraction peaks, the structure could not be determined. However, the density considerations suggest that this large unit cell should have at least 22 formula units per unit cell and this would imply at least

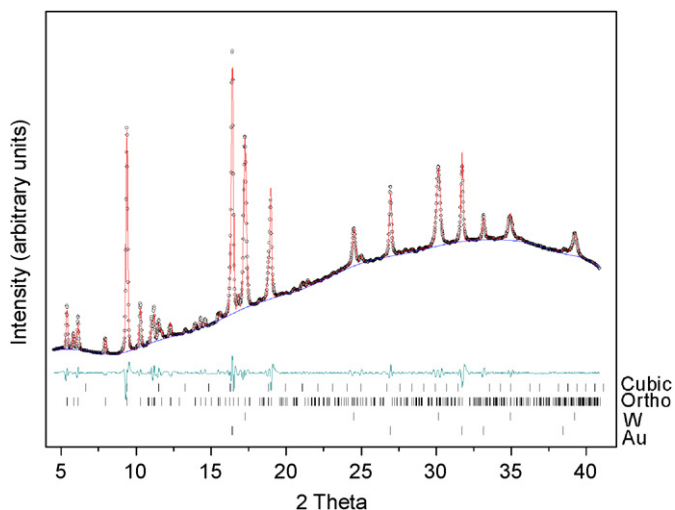


Fig. 3. Le Bail profile fitting of the diffraction pattern of  $Zn(CN)_2$  at 1.3 GPa with four phases i.e., gold pressure marker, tungsten gasket, orthorhombic high pressure phase and ambient cubic phase. The coexistence of the parent and the daughter phases implies the phase transition at  $\sim 1$  GPa to be of first order.

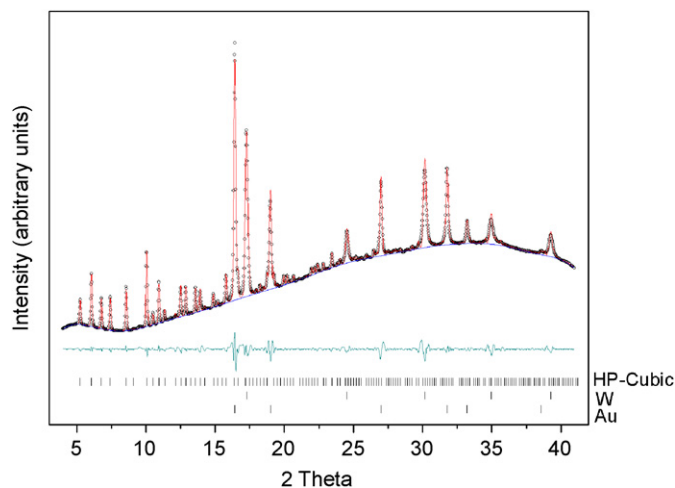


Fig. 4. Le Bail profile fitting of the observed diffraction pattern of  $Zn(CN)_2$  at 2.5 GPa employing three phases i.e., gold pressure marker, tungsten gasket and cubic high pressure phase.

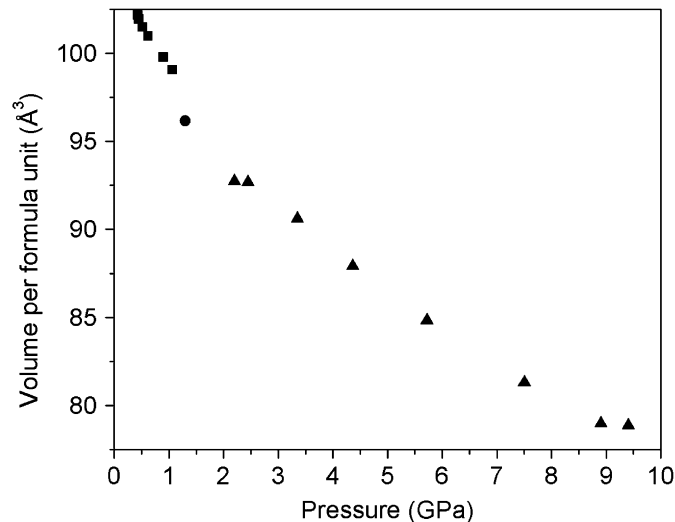


Fig. 5. Variation of volume per formula-unit with pressures under hydrostatic conditions in three different phases, solid squares represent ambient cubic phase (with formula units/cell ( $Z = 2$ )), solid diamond represents high pressure orthorhombic phase ( $Z = 4$ ) and solid triangles represent high pressure cubic phase ( $Z = 22$ ).

$\sim 4\%$  volume reduction per formula unit across the phase transition. Extinction conditions give two probable space groups viz.,  $P2_13$  or  $P4_232$ . However, multiplicities of site positions of  $P2_13$  space group indicate that there should be 20 formula units per unit cell. This will lead to higher volume per formula units compared to the low pressure phase, which is unphysical. These observations suggest that high pressure cubic phase may belong to  $P4_232$  space group. This space group can also rationalize the existence of 22 formula units per unit cell. This high pressure phase remained stable up to  $\sim 9$  GPa. The variation of volume/formula-unit, as deduced from the diffraction data up to  $\sim 9$  GPa, is shown in Fig. 5.

Beyond  $\sim 9$  GPa, all the diffraction peaks started showing broadening concomitant with the decrease in the intensities. The observation of a broad hump at  $2\theta \sim 14^\circ$  implies that the structure becomes increasingly disordered at higher pressures. By  $\sim 11$  GPa almost all the diffraction peaks of the sample vanished leaving behind only the hump and the diffraction peaks from the

pressure marker (gold) and the gasket (tungsten). This indicates that  $\text{Zn}(\text{CN})_2$  transforms to an amorphous phase at  $\sim 11$  GPa. To test whether this amorphous phase transforms to any crystalline phase if overdriven, pressure was further raised up to  $\sim 14$  GPa. However, our results show that it remained amorphous. On release of pressure the diffraction pattern did not show any reappearance of the crystalline structure, establishing irreversible PIA of  $\text{Zn}(\text{CN})_2$ .

Before we present the results under non-hydrostatic pressure conditions, it would be useful to state here a few general points. As the non-hydrostatic conditions in a DAC are necessarily due to the heterogeneous stress distribution, it is likely that the diffraction peaks would be broader in this case. While, in principle, non-hydrostatic stresses can change the nature of phase transformation ([4,5,29] and reference therein), one should also take care of the fact that the heterogeneity in stress distribution can bring about multiple phase co-existence. However, when the size of the grains in the powdered sample is orders of magnitude smaller than the dimensions of the sample contributing to diffraction pattern, one may expect a reasonable degree of reproducibility in the experimental results. With these general points, we present the diffraction patterns for  $\text{Zn}(\text{CN})_2$  under non-hydrostatic pressure conditions in Fig. 6. In this case the initial cubic phase persisted up to  $\sim 2$  GPa, indicating somewhat extended stability region of the cubic phase than under the hydrostatic pressures. On further increase of pressure diffraction peaks continued to broaden. At  $\sim 3.5$  GPa diffraction pattern showed new, but broad, diffraction peaks at 4.75, 4.28, 3.65 and

2.68 Å. Due to the broad nature of these peaks, the diffraction pattern could not be indexed [30]. However, careful analysis shows that the broad peaks under non-hydrostatic pressures are not the overlapped broadened peaks of hydrostatic experiments. Thus the new phase observed under non-hydrostatic stresses is distinct from that obtained under hydrostatic conditions. At still higher pressures, the diffraction peaks became very broad and our data suggests that by  $\sim 10.5$  GPa the sample became substantially disordered and remained so upto  $\sim 11.7$  GPa. On release of pressure, the sample remained in the disordered state i.e., did not revert to any crystalline phase, much like in the hydrostatic experiments. We should note that the disordered phase under non-hydrostatic conditions still has some persistent diffractive features at  $\sim 11.7$  GPa, at variance with the results obtained under hydrostatic conditions where the sample became essentially amorphous at  $\sim 11$  GPa. These results imply that under non-hydrostatic conditions, the structure may not be as disordered as under hydrostatic pressures and this difference may have its roots in the fact that the preceding structures are different in these two cases [31]

Several high pressure studies have earlier been carried out on various cyanide compounds [32–34]. Raman investigations on  $\text{K}_2\text{Hg}(\text{CN})_4$  show several phase transitions, proposed to be related to the modifications of tetrahedra as well as bending of C–Hg–C and Hg–C–N angles [32].  $\text{Hg}(\text{CN})_2$  has substantially different structure but still undergoes several high pressure phase transitions [33]. As mentioned in Section 1, earlier high pressure investigations on  $\text{Zn}(\text{CN})_2$  suggested PIA of this compound at  $\sim 1.6$  GPa [23]. However, due to the usage of laboratory X-ray source, the diffraction pattern had poor signal/noise ratio and hence the present study supersedes those results.

The studies carried out so far do not elucidate the mechanism of PIA of  $\text{Zn}(\text{CN})_2$ . We may mention that in some materials such as in ice and quartz, softening of a transverse acoustic branch (and hence an appropriate elastic constant) has been proposed to be the mechanism for the PIA [35–37]. In such cases amorphous phase may be viewed as an assemblage of a large number of incommensurate states [38]. Such a mechanism for the amorphization would imply that this transformation should get completed over a very small range of pressure, if not at a specific value of the pressure. For  $\text{Zn}(\text{CN})_2$ , the amorphous/disordered phases arise over a pressure range of  $\sim 2$  GPa, suggesting that softening of elastic constants may not be the mechanism for  $\text{Zn}(\text{CN})_2$ . In any case, for such a mechanism for  $\text{Zn}(\text{CN})_2$ , the computed elastic modulus must be shown to vanish in the phase just preceding the amorphous phase, necessitating its unambiguous structural determination. A more general interpretation of PIA is that the amorphous state is a kinetically preferred state brought about by the inability of the compound to reach a higher coordinated crystalline state [10]. A recent investigation on  $\text{Zr}(\text{WO}_4)_2$  suggests a similar mechanism is operative even for other compounds showing NTE (which have a large number of low frequency modes) [39]. This should encourage further studies on  $\text{Zn}(\text{CN})_2$  at high pressures and temperatures.

In conclusion, under the hydrostatic pressures, we have observed three phase transformations i.e., cubic  $\rightarrow$  orthorhombic  $\rightarrow$  cubic-II  $\rightarrow$  amorphous. PIA is observed to occur at  $\sim 11$  GPa, at variance with the results published earlier where it was claimed to take place at  $\sim 1.6$  GPa [21,23]. In contrast, under non-hydrostatic conditions,  $\text{Zn}(\text{CN})_2$  undergoes two structural transformations i.e., cubic phase to a partially disordered crystalline phase followed by an evolution to a substantially disordered phase. Moreover, the disordered phase in this case is different from that obtained under hydrostatic conditions.

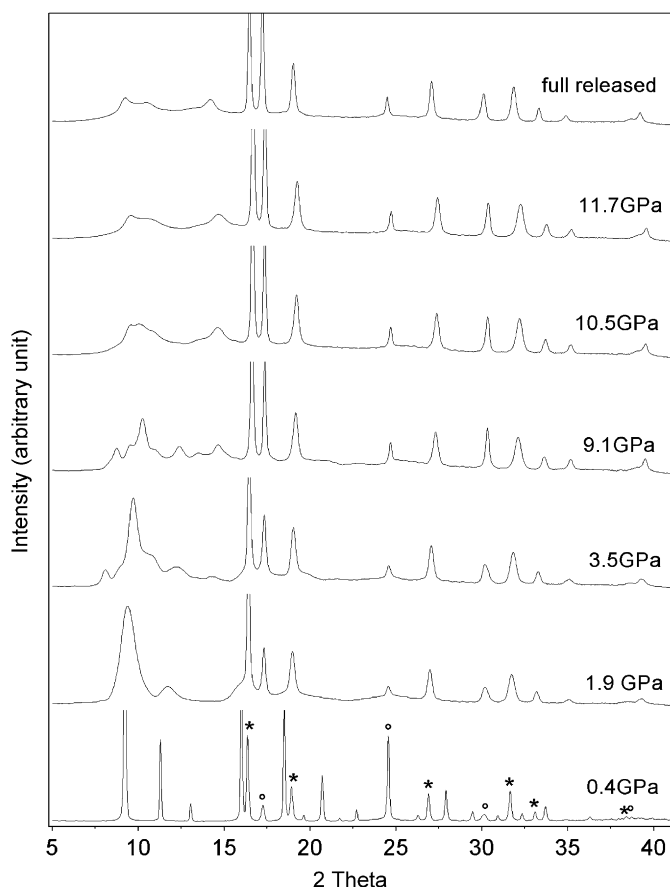


**Fig. 6.** X-ray diffraction patterns of  $\text{Zn}(\text{CN})_2$  at a few representative pressures under non-hydrostatic conditions. Open circles and asterisks represent the diffraction peaks from tungsten gasket and gold pressure marker, respectively.

## Acknowledgment

Authors are thankful to Dr. Nandini Garg for her help during experiments.

## Appendix A. Supporting Information

Supplementary data associated with this article can be found in the online version at doi:10.1016/j.jssc.2008.09.026.

## References

- [1] J.S.O. Evans, T.A. Mary, T. vogt, M.A. Subramanian, A.W. Sleight, *Chem. Mater.* 8 (1996) 2809.
- [2] M.G. Tucker, A.L. Goodwin, M.T. Dove, D.A. Keen, S.A. Wells, J.S.O. Evans, *Phys. Rev. Lett.* 95 (2005) 255501.
- [3] A.W. Sleight, *Curr. Opin. Solid State Mater. Sci.* 3 (1998) 128.
- [4] S.K. Sikka, *J. Phys.: Condens. Matter* 16 (2004) S1033.
- [5] G.D. Barrera, J.A.O. Bruno, T.H.K. Barron, N.L. Allan, *J. Phys.: Condens. Matter* 17 (2005) R217.
- [6] C.N. Chu, N. Saka, N.P. Suh, *Mater. Sci. Eng.* 95 (1987) 303.
- [7] N. Garg, C. Murli, A.K. Tyagi, S.M. Sharma, *Phys. Rev. B* 72 (2005) 064106.
- [8] N. Garg, V. Panchal, A.K. Tyagi, S.M. Sharma, *J. Solid Stat. Chem.* 178 (2005) 998.
- [9] S. Carlson, A.M.K. Anderson, *J. Appl. Cryst.* 34 (2001) 7.
- [10] S.M. Sharma, S.K. Sikka, *Prog. Mater. Sci.* 40 (1996) 1.
- [11] J.S.O. Evans, Z. Hu, J.D. Jorgensen, D.N. Argyriou, S. Short, A.W. Sleight, *Science* 275 (1997) 61.
- [12] R.J. Speedy, *J. Phys.: Condens. Matter* 8 (1996) 10907.
- [13] D. Williams, D.E. Parting, F.J. Lincoln, J. Kouvetakis, M. O'Keeffe, *J. Solid State Chem.* 134 (1997) 164.
- [14] J.W. Zwanziger, *Phys. Rev. B* 76 (2007) 52102.
- [15] B.F. Hoskins, R. Robson, *J. Am. Chem. Soc.* 112 (1990) 1546.
- [16] R.J. Angel, B. Maciej, Z. Jing, G. Diego, S.D. Jacobson, *J. Appl. Cryst.* 40 (2007) 26.
- [17] K.W. Chapman, P.J. Chupas, C.J. Kepert, *J. Am. Chem. Soc.* 127 (2005) 15630.
- [18] K.W. Chapman, M. Hagen, C.J. Kepert, P. Manuel, *Physica B* 385 (2006) 60.
- [19] A.L. Goodwin, C.J. Kepert, *Phys. Rev. B* 71 (2005) 140301.
- [20] A.L. Goodwin, *Phys. Rev. B* 74 (2006) 134302.
- [21] T.R. Ravindran, A.K. Arora, T.N. Sairam, *J. Raman Spectroscopy* 38 (2007) 283.
- [22] K.W. Chapman, P.J. Chupas, *J. Am. Chem. Soc.* 129 (2007) 10090.
- [23] T.R. Ravindran, A.K. Arora, S. Chandra, M.C. Valsakumar, N.V. Chandra Shekar, *Phys. Rev. B* 76 (2007) 054302.
- [24] A. Dewaele, P. Loubeyre, M. Mezouar, *Phys. Rev. B* 70 (2004) 94112.
- [25] A.P. Hammersley, S.O. Svensson, M. Hanfland, A.N. Fitch, D. Hauserman, *High Pressure Res.* 14 (1996) 235.
- [26] A.C. Larson, R.B. Von Dreele, Los Alamos National Laboratory Report LAUR, 86, 2000.
- [27] R. Shirley, *Crysfire*, 2004.
- [28] Jean Laugier et Bernard Bochu <<http://www.inpg.fr/LMGP>> or <<http://www.ccp14.ac.uk/tutorial/lmgp/>>.
- [29] N. Garg, S.M. Sharma, *J. Phys.: Condens. Matter* 19 (2007) 456201.
- [30] The observed pressure induced variations of the *d*-spacings under non-hydrostatic pressures and their comparison with the corresponding variations under hydrostatic pressures has been submitted as supplementary information.
- [31] In principle, one cannot rule out the possibility of pressure medium (alcohol mixture) reacting irreversibly with Zn(CN)<sub>2</sub> at high pressures. However, we feel that it is unlikely as at low pressures the X-ray diffraction patterns as well as Raman spectra are same as that of the initial cubic phase, and visual observations show that at high pressures the nature of powdered sample stays the same as loaded initially. In addition, at higher pressures the new phases are expected to be denser than the initial phases.
- [32] P.T.T. Wong, *Phys. Rev. B* 23 (1981) 375.
- [33] D.M. Adams, P.D. Hatton, *J. Phys. C: Solid Stat. Phys.* 16 (1983) 3349.
- [34] G. Dehnicke, K. Dehnicke, H. Ahsbahs, E. Hellner, *Ber. Bunsen. Phys. Chem.* 78 (1974) 1010.
- [35] Th. Strässle, A.M. Saitta, S. Klotz, M. Braden, *Phys. Rev. Lett.* 93 (2004) 225901.
- [36] J.S. Tse, D.D. Klug, C.A. Tulk, I. Swainson, E.C. Svensson, C.K. Loong, V. Shpakov, V.R. Belosludov, R.V. Belosludov, Y. Kawazoe, *Nature (London)* 400 (1999) 647.
- [37] K. Umemoto, R.M. Wentzcovitch, S. Baroni, S. Gironcoli, *Phys. Rev. Lett.* 92 (2004) 105502.
- [38] S.M. Sharma, *Indian J. Pure Appl. Phys.* 33 (1995) 562.
- [39] D.A. Keen, A.L. Goodwin, M.G. Tucker, M.T. Dove, J.S.O. Evans, W.A. Crichton, M. Brunelli, *Phys. Rev. Lett.* 98 (2007) 225501.